

Ruthenium bipyridyl compounds with two terminal alkynyl ligands

Christopher J. Adams,^{*a} Lucy E. Bowen,^a Mark G. Humphrey,^b Joseph P. L. Morrall,^b Marek Samoc^c and Lesley J. Yellowlees^d^a School of Chemistry, University of Bristol, Bristol, UK, BS8 1TS. E-mail: chcja@bris.ac.uk^b Department of Chemistry, Australian National University, Canberra, Australia, ACT 0200. E-mail: Mark.Humphrey@anu.edu.au^c Laser Physics Centre, Research School of Physical Sciences and Engineering, Australian National University, Canberra, Australia, ACT 0200^d School of Chemistry, Joseph Black Building, West Mains Road, Edinburgh, UK, EH9 3JJ. E-mail: l.j.yellowlees@ed.ac.uk

Received 28th July 2004, Accepted 6th October 2004

First published as an Advance Article on the web 9th November 2004

Compounds of the form $\text{Ru}(\text{X}_2\text{bipy})(\text{PPh}_3)_2(-\text{C}\equiv\text{CC}_6\text{H}_4\text{NO}_2-p)_2$ ($\text{X}_2\text{bipy} = 4,4'-\text{X}_2-2,2'$ -bipyridine, $\text{X} = \text{Me}$ **3a**, **Br** **3b**, **I** **3c**) have been synthesised from the mono-alkynyl precursors $\text{Ru}(\text{X}_2\text{bipy})(\text{PPh}_3)_2(-\text{C}\equiv\text{CC}_6\text{H}_4\text{NO}_2-p)\text{Cl}$ ($\text{X} = \text{Me}$ **2a**, **Br** **2b**, **I** **2c**); the former are the first ruthenium bis-alkynyl compounds that also contain a bipyridyl ligand. Spectroelectrochemical investigation of **3a** shows that the metal is readily oxidised to form the ruthenium(III) compound **3a⁺**, and will also undergo a single-electron reduction at each nitro group to form **3a²⁻**. ESR and UV/visible spectra of these redox congeners are presented. We also report the synthesis of $[\text{Ru}(\text{Me}_2\text{bipy})(\text{PPh}_3)_2(-\text{C}\equiv\text{CBu}^t(\text{N}\equiv\text{N}))][\text{PF}_6]$ **4** during the attempted synthesis of $\text{Ru}(\text{Me}_2\text{bipy})(\text{PPh}_3)_2(-\text{C}\equiv\text{CBu}^t)_2$, and report its X-ray crystal structure and IR spectrum. X-Ray crystal structures of **3b** and **3c** (as two different solvates) are presented, and the nature of the intermolecular interactions seen therein is discussed. Z-Scan measurements on $\text{Ru}(\text{Me}_2\text{bipy})(\text{PPh}_3)_2(-\text{C}\equiv\text{CR})\text{Cl}$ ($\text{R} = \text{C}_6\text{H}_4\text{NO}_2-p$ **2a**, Bu^t , Ph , $\text{C}_6\text{H}_4\text{Me}$) are also reported, and show that $\text{Ru}(\text{Me}_2\text{bipy})(\text{PPh}_3)_2(-\text{C}\equiv\text{CR})\text{Cl}$ ($\text{R} = \text{C}_6\text{H}_4\text{NO}_2-p$ **2a**, Ph) exhibit moderate third-order non-linearities.

Introduction

We have recently published the first results from our investigation into the synthesis and properties of ruthenium-alkynyl compounds that also contain a bipyridyl ligand,¹ stimulated by an analogy between them and a class of platinum compounds that have received extensive investigation over the past four years. Such bipyridyl-platinum-bis(alkynyl) compounds have been shown to luminesce strongly from a ³MLCT excited state in both frozen and fluid solution, and have also recently demonstrated vapoluminescence and interesting interactions with solvent molecules in the crystal lattice.² The same arrangement of bipyridyl and alkynyl ligands can be envisaged in the equatorial positions of an octahedral ruthenium centre, with secondary ligands occupying the axial positions. Such d⁶ octahedral ruthenium compounds could display the same optoelectronic properties as the d⁸ square-planar platinum species, as well as additional properties such as redox-switchable behaviour and tunability through the alteration of the axial ligands.

Thus far, we have reported on compounds of the general formula $\text{Ru}(\text{Me}_2\text{bipy})(\text{PPh}_3)_2(-\text{C}\equiv\text{CR})\text{Cl}$ ($\text{Me}_2\text{bipy} = 4,4'$ -dimethyl-2,2'-bipyridine; $\text{R} = \text{Bu}^t$, Ph , $\text{C}_6\text{H}_4\text{Me}$); that is, mono-alkynyl species. These compounds are synthesised from the corresponding dichloride precursor *via* an intermediate cationic vinylidene compound, which is formed when one of the chloride ligands is replaced with a terminal alkyne, and which may then be deprotonated to yield the alkynyl complex. Although the spectra of these mono-alkynyl compounds possess the same MLCT bands as the aforementioned platinum compounds they do not appear to show the same emissive behaviour, which could be because of the presence of the chloride ligands, which dissociate to some extent in solution and may quench any emission. The compounds do however show redox-switchable optical properties, changing colour as the lowest energy band in the UV/visible spectrum changes from MLCT to LMCT upon oxidation from Ru(II) to Ru(III).¹

The current work reports the results of our investigations of the synthesis of bis(alkynyl) compounds of the form

$\text{Ru}(\text{Me}_2\text{bipy})(\text{PPh}_3)_2(-\text{C}\equiv\text{CR})_2$ from the mono(alkynyl) compounds mentioned above. This has been attempted in the same way as before, *via* intermediate vinylidene compounds, although a one-pot procedure has been developed so that these vinylidenes do not need to be isolated. Success has been achieved with $\text{R} = \text{C}_6\text{H}_4\text{NO}_2-p$, but not with $\text{R} = \text{Bu}^t$ or $\text{C}_6\text{H}_4\text{Me}-p$.

Experimental

General information

All new compounds except **4** are air stable in the solid state and reasonably air stable in solution, but standard inert-atmosphere techniques were used throughout. All solvents were purified using an Anhydrous Engineering Grubbs-type solvent system.³ The starting materials $\text{Ru}(\text{PPh}_3)_3\text{Cl}_2$,⁴ $\text{Ru}(\text{Me}_2\text{bipy})(\text{PPh}_3)_2\text{Cl}_2$ **1a**,⁵ $\text{Ru}(\text{Me}_2\text{bipy})(\text{PPh}_3)_2(-\text{C}\equiv\text{CR})\text{Cl}$ ($\text{R} = \text{Bu}^t$, Ph , p - $\text{C}_6\text{H}_4\text{Me}$),¹ 4,4'-dibromo-2,2'-bipyridine (**Br**₂bipy),⁶ 4,4'-dinitro-2,2'-bipyridine *N,N'*-dioxide⁷ and *p*-nitrophenylacetylene⁸ were prepared by literature methods, and all other chemicals were used as purchased. IR and UV/visible spectra were recorded in dichloromethane solution on a Perkin-Elmer 1600 series FTIR spectrometer and a Perkin-Elmer λ-19 spectrophotometer respectively. Cyclic voltammetry was carried out under an atmosphere of nitrogen using the standard three-electrode configuration, with platinum working and counter electrodes, an SCE reference electrode, dichloromethane as solvent, 0.1 M $[\text{Bu}_4\text{N}][\text{PF}_6]$ as electrolyte and FeCp_2 or FeCp^*_2 as internal calibrant, and a substrate concentration of approximately 1 mM. All potentials are reported *vs.* the SCE reference electrode, against which the $\text{FeCp}_2/[\text{FeCp}_2]^+$ couple comes at 0.46 V and $\text{FeCp}^*_2/[\text{FeCp}^*_2]^+$ is -0.02 V.⁹ X-Band ESR spectra of **2a⁺** and **3a⁺** were recorded at the University of Bristol on a Bruker ESP300E spectrometer in 2 : 1 thf-CH₂Cl₂ at 110 K, and that of **3a²⁻** at the University of Edinburgh on a Bruker ER200D spectrometer. NMR spectra were recorded in CDCl₃ (unless otherwise stated) on a JEOL ECP300 spectrometer, at 300 MHz (¹H) and 121 MHz (³¹P), and referenced to external TMS and

external 85% H_3PO_4 , respectively. UV/visible spectroelectrochemical measurements were performed in CH_2Cl_2 at 243 K using a locally constructed OTTE (optically transparent thin-layer electrode) cell in a Perkin-Elmer λ -19 spectrophotometer, as described previously.¹⁰ Microanalyses were carried out by the staff of the Microanalytical Service of the School of Chemistry at the University of Bristol.

Syntheses

4,4'-Diamino-2,2'-bipyridine. This was synthesised by the reported procedure,¹¹ but isolated differently. In a typical example, 3.83 g (0.013 mol) of 4,4'-dinitro-2,2'-bipyridine *N,N'*-dioxide and 1 g of 10% palladium on carbon were suspended in 100 cm^3 of degassed ethanol. A solution of hydrazine monohydrate (4 cm^3) in ethanol (20 cm^3) was added dropwise to this over the course of an hour, and the solution was then refluxed for 8 h. After cooling it was filtered through Celite (which was then washed with more ethanol), and the combined ethanol solutions were reduced in volume to approximately 100 cm^3 , using a rotary evaporator with a hot water-bath. At this stage the solution should still be clear; any yellow precipitate can be redissolved by addition of a little more ethanol and further heating. 50 cm^3 of distilled water was then added, and the solution again reduced to about 100 cm^3 . At this point, slow addition of a further 100 cm^3 of distilled water caused the product to form as a white crystalline solid; the solution was refrigerated overnight to ensure complete crystallisation. Following isolation by filtration, washing with distilled water, and drying, the product was isolated as a white (lit¹¹: yellow) solid (1.76 g, 69%). ¹H NMR (d_6 -DMSO) δ : 6.01 (4H, s, NH_2), 6.41 (2H, dd, $^3J_{\text{HH}} = 5.5$ Hz, $^4J_{\text{HH}} = 2.3$ Hz, H_5), 7.51 (2H, d, $^3J_{\text{HH}} = 2.3$ Hz, H_3), 8.00 (2H, d, $^4J_{\text{HH}} = 5.5$ Hz, H_6). Anal. Calc. for $\text{C}_{10}\text{H}_{10}\text{N}_4$: C 64.50; H 5.41; N 30.09%. Found: C 64.40; H 5.58; N 30.29%.

4,4'-Diiodo-2,2'-bipyridine (I₂bipy). This compound was prepared from 4,4'-diamino-2,2'-bipyridine in a manner analogous to the preparation of 4-iodopyridine from 4-aminopyridine.¹² Thus, 4,4'-diamino-2,2'-bipyridine (0.9 g, 4.5 mmol) was suspended in 48% aqueous HBF_4 (25 cm^3) and cooled to -10 °C. To the resulting slurry was added, portionwise over the course of about 1 h, powdered sodium nitrite (1.3 g, 18.8 mmol), at such a rate that no nitric oxide evolution was detected. After a further 15 min stirring, the precipitate of diazonium salt was isolated by suction filtration, but not allowed to dry out. This was then added, portionwise over the course of about 30 min, to a cooled (-10 °C) solution of potassium iodide (5.1 g, 30.7 mmol) in an acetone–water (40 : 60, 100 cm^3) solution. The reaction was then stirred for 30 min, being allowed to warm to room temperature, giving a yellow–brown suspension. This was neutralised by adding aqueous sodium carbonate, and then a little aqueous sodium thiosulfate solution was added to decolorise the solution phase. Extraction with dichloromethane (4×50 cm^3) gave a yellow solution, which was dried over magnesium sulfate and treated with activated carbon. Following filtration through an alumina pad (2 cm diameter \times 2 cm depth), the solvent was removed under vacuum to give the crude product. This was redissolved in hot ethanol, treated again with activated carbon, and filtered hot through Celite. Upon cooling and storage at -10 °C the compound formed as a white crystalline solid, which was isolated by filtration and dried (0.66 g, 1.61 mmol, 33%). ¹H NMR δ : 7.63 (2H, dd, $^3J_{\text{HH}} = 5.4$ Hz, $^4J_{\text{HH}} = 1.9$ Hz, H_5), 8.23 (2H, d, $^3J_{\text{HH}} = 5.4$ Hz, H_6), 8.73 (2H, d, $^4J_{\text{HH}} = 1.9$ Hz, H_3). Anal. Calc. for $\text{C}_{10}\text{H}_6\text{N}_2\text{I}_2$: C 29.44; H 1.48; N 6.87%. Found: C 29.73; H 1.52; N 6.88%.

Ru(Br₂bipy)(PPh₃)₂Cl₂ 1b. 0.043 g (0.14 mmol) of 4,4'-dibromo-2,2'-bipyridine and 0.125 g (0.13 mmol) of $\text{RuCl}_2(\text{PPh}_3)_3$ were stirred for 90 min in 10 cm^3 of CH_2Cl_2 to give a deep purple solution. To this was slowly added 30 cm^3 of hexane, and the solution was refrigerated overnight to yield

deep purple crystals of the desired product as a dichloromethane solvate. These were isolated by filtration, washed with hexane and dried to give 0.112 g (0.102 mmol, 74%) of product. ¹H NMR δ : 6.52 (2H, dd, $^3J_{\text{HH}} = 6.4$ Hz, $^4J_{\text{HH}} = 2.2$ Hz, H_5); 7.04–7.20 (18H, m, Ph); 7.46–7.54 (12H, m, Ph); 7.63 (2H, d, $^4J_{\text{HH}} = 2.2$ Hz, H_3); 8.58 (2H, d, $^3J_{\text{HH}} = 6.4$ Hz, H_6). ³¹P NMR δ : 22.0. Anal. Calc. for $\text{C}_{46}\text{H}_{36}\text{N}_2\text{P}_2\text{Cl}_2\text{Br}_2\text{Ru}\cdot\text{CH}_2\text{Cl}_2$: C 51.53; H 3.50; N 2.66%. Found: C 51.71; H 3.54; N 2.65%. $\lambda_{\text{max}}/\text{nm}$: 532 ($\epsilon = 3167$ M^{-1} cm^{-1}), 368 (7421), 306 (17065), 272 (34040). $E^\circ = 0.58$ V.

Ru(I₂bipy)(PPh₃)₂Cl₂ 1c. 0.074 g (0.18 mmol) of 4,4'-diiodo-2,2'-bipyridine and 0.172 g (0.13 mmol) of $\text{RuCl}_2(\text{PPh}_3)_3$ were stirred for 45 min in 10 cm^3 of CH_2Cl_2 to give a deep purple solution. To this was slowly added 20 cm^3 of hexane, and the solution was refrigerated overnight to yield deep purple crystals of the desired product. These were isolated by filtration, washed with hexane and dried to give 0.094 g (0.085 mmol, 47%) of product. ¹H NMR δ : 6.68 (2H, dd, $^3J_{\text{HH}} = 6.2$ Hz, $^4J_{\text{HH}} = 1.8$ Hz, H_5), 7.03–7.20 (18H, m, Ph), 7.42–7.54 (12H, m, Ph), 7.76 (2H, d, $^4J_{\text{HH}} = 1.8$ Hz, H_3), 8.39 (2H, d, $^3J_{\text{HH}} = 6.2$ Hz, H_6). ³¹P NMR δ : 22.0. Anal. Calc. for $\text{C}_{46}\text{H}_{36}\text{N}_2\text{P}_2\text{Cl}_2\text{I}_2\text{Ru}$: C 50.02; H 3.29; N 2.54%. Found: C 50.17; H 3.29; N 2.50%. $\lambda_{\text{max}}/\text{nm}$: 531 ($\epsilon = 4174$ M^{-1} cm^{-1}), 371 (9996), 311 (21732), 272 (43413). $E^\circ = 0.57$ V.

Ru(Me₂bipy)(PPh₃)₂(-C \equiv CC₆H₄NO₂-*p*)Cl₂ 2a. 0.304 g of $\text{Ru}(\text{Me}_2\text{bipy})(\text{PPh}_3)_2\text{Cl}_2$ **1a** (0.34 mmol), 0.070 g of *p*-nitrophenylacetylene (0.48 mmol) and 0.121 g (0.34 mmol) of TiPF_6 were stirred for 2 h in 10 cm^3 of CH_2Cl_2 . To the resulting orange solution with a white precipitate was added 0.3 g (2.1 mmol) of potassium carbonate, and the solution was allowed to stir overnight. The resulting purple solution containing a white precipitate was filtered, and the residual solid washed with a further 2×5 cm^3 portions of CH_2Cl_2 . 100 cm^3 of diethyl ether was then added to the combined solutions, and overnight refrigeration yielded **2a** as a purple–brown solid with a green iridescence (0.238 g, 0.24 mmol, 70%). ¹H NMR δ : 2.20, 2.34 (each 3H, s, Me); 5.91 (1H, d, $^3J_{\text{HH}} = 4.7$ Hz, H_5); 6.64 (1H, d, $^3J_{\text{HH}} = 4.7$ Hz, H_5); 6.80 (2H, d, $^3J_{\text{HH}} = 8.8$ Hz, C_6H_4); 7.00–7.17 (18H, m, Ph); 7.37 (1H, s, H_3); 7.52–7.61 (13H, m, Ph and H_3); 7.96 (2H, d, $^3J_{\text{HH}} = 8.8$ Hz, C_6H_4); 8.02 (1H, d, $^3J_{\text{HH}} = 5.8$ Hz, H_6); 8.87 (1H, d, $^3J_{\text{HH}} = 5.8$ Hz, H_6). ³¹P NMR δ : 30.5. Anal. Calc. for $\text{C}_{56}\text{H}_{46}\text{N}_3\text{P}_2\text{Cl}_2\text{RuO}_2$: C 67.84; H 4.68; N 4.24%. Found: C 67.66; H 4.90; N 4.32%. FT-IR $\nu(\text{C}\equiv\text{C})/\text{cm}^{-1}$: 2043s, 2014 sh. $\lambda_{\text{max}}/\text{nm}$: 515 ($\epsilon = 22552$ M^{-1} cm^{-1}), 332sh (11920), 298 (26923), 277 (36485). $E^\circ = 0.39, -1.23$ V.

Ru(Br₂bipy)(PPh₃)₂(-C \equiv CC₆H₄NO₂-*p*)Cl₂ 2b. 0.185 g of $\text{Ru}(\text{Br}_2\text{bipy})(\text{PPh}_3)_2\text{Cl}_2\cdot\text{CH}_2\text{Cl}_2$ **1b** (CH_2Cl_2 0.17 mmol), 0.064 g of TiPF_6 (0.18 mmol) and 0.040 g of *p*-nitrophenylacetylene (0.27 mmol) were stirred for 2 h in 10 cm^3 of CH_2Cl_2 to give an orange–brown solution. To this was added 0.180 g of K_2CO_3 (1.30 mmol), and the reaction stirred for a further 20 h to give a red–purple solution. This was filtered through a filter-paper tipped cannula, and the residual solid washed with a further 5 cm^3 of CH_2Cl_2 . 35 cm^3 of hexane were added to the combined solutions, which were then stored at 4 °C for 48 h, after which time filtration allowed the isolation of the desired product as a microcrystalline brown solid, which was washed with hexane and dried under vacuum to give 0.141 g of product (0.13 mmol, 75%). ¹H NMR δ : 6.27 (1H, dd, $^3J_{\text{HH}} = 6.2$ Hz, $^4J_{\text{HH}} = 2.2$ Hz, H_5); 6.74 (2H, d, $^3J_{\text{HH}} = 8.8$ Hz, C_6H_4); 6.97 (1H, dd, $^3J_{\text{HH}} = 6.2$ Hz, $^4J_{\text{HH}} = 1.9$ Hz, H_5); 7.02–7.18 (18H, m, Ph); 7.48–7.58 (12H, m, Ph); 7.65 (1H, d, $^4J_{\text{HH}} = 2.2$ Hz, H_3); 7.80 (1H, d, $^4J_{\text{HH}} = 1.9$ Hz, H_3); 7.96 (2H, d, $^3J_{\text{HH}} = 8.8$ Hz, C_6H_4); 8.06 (1H, d, $^3J_{\text{HH}} = 6.6$ Hz, H_6); 8.88 (1H, d, $^3J_{\text{HH}} = 6.0$ Hz, H_6). ³¹P NMR δ : 28.5. Anal. Calc. for $\text{C}_{54}\text{H}_{40}\text{Br}_2\text{ClN}_3\text{O}_2\text{P}_2\text{Ru}$: C, 57.85; H 3.60; N 3.75%. Found: C, 57.53; H 3.63; N 3.79%. FT-IR $\nu(\text{C}\equiv\text{C})/\text{cm}^{-1}$: 2048s, 2011sh. $\lambda_{\text{max}}/\text{nm}$: 518 ($\epsilon = 20442$ M^{-1} cm^{-1}), 362 (8219), 306 (25126), 276 (38234). $E^\circ = 0.56$ V.

Ru(I₂bipy)(PPh₃)₂(-C≡CC₆H₄NO₂-*p*)Cl 2c. 0.107 g of Ru(I₂bipy)(PPh₃)₂Cl₂ **1c** (0.097 mmol), 0.034 g of TlPF₆ (0.097 mmol) and 0.028 g of *p*-nitrophenylacetylene (0.19 mmol) were stirred for 4 h in 10 cm³ of CH₂Cl₂ to give an orange-brown solution. To this was added 0.100 g of K₂CO₃ (0.72 mmol), and the reaction stirred for a further 20 h to give a red-purple solution. This was filtered through a filter-paper tipped cannula, and the residual solid washed with a further 5 cm³ of CH₂Cl₂. 40 cm³ of hexane were added to the combined solutions, which were then stored at 4 °C for 24 h, after which time filtration allowed the isolation of the desired product as a microcrystalline brown solid, which was washed with hexane and dried under vacuum to give 0.062 g of product (0.051 mmol, 52%). ¹H NMR δ: 6.42 (dd, *J*_{HH} = 6.2 Hz, 1.8 Hz, 1H, H₅); 6.83 (d, *J*_{HH} = 8.8 Hz, 2H, C₆H₄); 7.04–7.21 (19H, m, Ph, H₅); 7.57–7.50 (12H, m, Ph); 7.79 (d, *J*_{HH} = 1.8 Hz, 1H, H_{3'}); 7.91 (d, *J*_{HH} = 6.2 Hz, 1H, H₆); 7.98 (m, 3H, H₃, C₆H₄); 8.71 (d, *J*_{HH} = 5.9 Hz, 1H, H₆). ³¹P NMR δ: 28.43. Anal. Calc. for C₃₄H₄₀I₂ClN₃O₂P₂Ru: C, 53.37; H 3.32; N 3.46%. Found: C, 53.70; H, 3.13; N, 3.34%. FT-IR ν(C≡C)/cm⁻¹: 2048s, 2012sh. λ_{max}/nm: 526 (ε = 20 392 M⁻¹ cm⁻¹), 369 (9197), 310 (26596), 275 (38722). E°' = 0.57 V.

Ru(Me₂bipy)(PPh₃)₂(-C≡CC₆H₄NO₂-*p*)₂ 3a. 0.150 g of Ru(Me₂bipy)(PPh₃)₂(Cl)(-C≡CC₆H₄NO₂-*p*) **2a** (0.15 mmol), 0.053 g of TlPF₆ (0.15 mmol) and 0.033 g of *p*-nitrophenylacetylene (0.22 mmol) were stirred for 48 h in 20 cm³ of CH₂Cl₂ to give an orange-brown solution. To this was added 0.150 g of K₂CO₃ (1.08 mmol), and the reaction stirred for a further 20 h to give a purple solution. This was filtered through Celite, and evaporated to dryness. The resulting purple solid was extracted into 20 cm³ of warm toluene, filtered through Celite, and then allowed to cool before being stored at -10 °C for 48 h. Decanting the liquid from the resulting mixture allowed the isolation of the desired product **3a** as dark crystals, which were washed with hexane and dried under vacuum to give 0.070 g of product (0.063 mmol, 42%). ¹H NMR δ: 2.31 (6H, s, Me); 6.39 (2H, d, ³*J*_{HH} = 5.7 Hz, H₅); 6.74 (4H, d, ³*J*_{HH} = 8.4 Hz, C₆H₄); 7.00–7.16 (18H, m, Ph); 7.54 (2H, s, H₃); 7.56–7.63 (12H, m, Ph); 7.92 (4H, d, ³*J*_{HH} = 8.4 Hz, C₆H₄); 8.35 (2H, d, ³*J*_{HH} = 5.7 Hz, H₆). ³¹P NMR δ: 36.4. Anal. Calc. for C₆₄H₅₀N₄P₂RuO₄: C 69.75; H 4.57; N 5.08%. Found: C 69.54; H 4.05; N 5.22%. FT-IR ν(C≡C)/cm⁻¹: 2010m, 2035s, 2056m. λ_{max}/nm: 507 (ε = 36896 M⁻¹ cm⁻¹), 330 (19856), 274 (39986). E°' = 0.42 V, -1.20 V.

Ru(Br₂bipy)(PPh₃)₂(-C≡CC₆H₄NO₂-*p*)₂ 3b. 0.086 g of Ru(Br₂bipy)(PPh₃)₂Cl(-C≡CC₆H₄NO₂-*p*) **2b** (0.08 mmol), 0.027 g of TlPF₆ (0.08 mmol) and 0.022 g of *p*-nitrophenylacetylene (0.15 mmol) were stirred for 2 days in 20 cm³ of CH₂Cl₂ to give an orange-brown solution. To this was added 0.086 g of K₂CO₃ (0.62 mmol), and the reaction stirred for a further 20 h to give a red-purple solution. This was filtered through Celite and evaporated to dryness, and then extracted into toluene. This toluene solution was filtered through Celite, and then reduced in volume on the rotary evaporator until solid material was observed around the side of the flask. This was redissolved by swirling, and the solution was stored at -10 °C for four days during which time the product was deposited as rectangular crystals. The solution was decanted from these, and they were then washed with hexane and dried under vacuum to give the desired product **3b** as brown crystals (0.044 g, 0.04 mmol, 47% yield). ¹H NMR δ: 6.72–6.78 (6H, m, C₆H₄ and H₅); 7.05–7.12 (12H, m, Ph); 7.55–7.22 (6H, m, Ph); 7.58–7.65 (12H, m, Ph); 7.82 (2H, d, ⁴*J*_{HH} = 2.2 Hz, H₃); 7.94 (4H, d, ³*J*_{HH} = 9.1 Hz, C₆H₄); 8.38 (2H, d, ³*J*_{HH} = 5.9 Hz, H₆). ³¹P NMR δ: 34.7. Anal. Calc. for C₆₂H₄₄Br₂N₄O₄P₂Ru: C, 60.45; H 3.60; N 4.55%. Found: C, 60.71; H 3.61; N 4.69%. FT-IR ν(C≡C)/cm⁻¹: 2060m, 2040s, 2010w. λ_{max}/nm: 523 (ε = 36255 M⁻¹ cm⁻¹), 306 (29993), 273 (43749). E°' = 0.55 V.

Ru(I₂bipy)(PPh₃)₂(-C≡CC₆H₄NO₂-*p*)₂ 3c. 0.072 g of Ru(I₂bipy)(PPh₃)₂Cl(-C≡CC₆H₄NO₂-*p*) **2c** (0.06 mmol), 0.021 g of TlPF₆ (0.06 mmol) and 0.017 g of *p*-nitrophenylacetylene (0.12 mmol) were stirred for 2 days in 20 cm³ of CH₂Cl₂ to give an orange-brown solution. To this was added 0.075 g of K₂CO₃ (0.54 mmol), and the reaction stirred for a further 2 d to give a purple solution. This was filtered through Celite and evaporated to dryness, and then extracted into toluene. This toluene solution was filtered through Celite, and then reduced in volume on the rotary evaporator until solid material was observed around the side of the flask. This was redissolved by swirling, and the solution was stored at -10 °C for two weeks, during which time the product was deposited as deep-purple crystals. The solution was decanted from these, and they were then washed with hexane and dried under vacuum to give 0.027 g (0.02 mmol, 29% yield {based on 2.5 toluene solvent molecules per molecule of **3c**}) of product. ¹H NMR δ: 6.78 (4H, d, ³*J*_{HH} = 8.8 Hz, C₆H₄); 6.92 (2H, dd, ³*J*_{HH} = 6.1 Hz, ⁴*J*_{HH} = 1.5 Hz, H₅); 7.26–7.08 (12H, m, Ph); 7.61–7.58 (18H, m, Ph); 7.94 (4H, d, ³*J*_{HH} = 8.8 Hz, C₆H₄); 7.98 (2H, d, ⁴*J*_{HH} = 1.8 Hz, H₃); 8.20 (2H, d, ³*J*_{HH} = 6.1 Hz, H₆). ³¹P NMR δ: 34.68. Anal. Calc. for C₆₂H₄₄I₂N₄O₄P₂Ru: C, 56.16; H 3.34; N 4.23%. Found: C, 56.36; H 3.22; N 4.13% (It was necessary to grind and thoroughly dry the sample in order to remove toluene and obtain satisfactory analysis). FT-IR ν(C≡C)/cm⁻¹: 2060m, 2040s, 2011w. λ_{max}/nm: 525 (ε = 34656 M⁻¹ cm⁻¹), 312 (30285), 271 (41447). E°' = 0.54 V.

[Ru(Me₂bipy)(PPh₃)₂(-C≡CBut)(N≡N)][PF₆] 4. Ru(Me₂bipy)(PPh₃)₂(-C≡CBut)Cl (0.053 g, 0.057 mmol) and TlPF₆ (0.020 g, 0.057 mmol) were stirred in 10 cm³ of nitrogen-saturated thf for 2 h to give an orange solution. This was filtered with a filter-paper tipped cannula, and 10 cm³ of hexane were added. Overnight refrigeration caused the formation of the desired product as red crystals, which were isolated by filtration, washed with hexane, and dried under vacuum, to give **4** as an orange-brown solid (0.038 g, 0.036 mmol, 63%). ¹H NMR δ: 1.17 (9H, s, Bu^t); 2.41 (6H, s, Me); 6.31 (1H, d, ³*J*_{HH} = 5.8 Hz, H₅); 6.38 (1H, d, ³*J*_{HH} = 4.8 Hz, H₅); 7.10–7.20 (12H, m, Ph); 7.20–7.30 (6H, m, Ph); 7.35–7.45 (12H, m, Ph); 8.13 (1H, s, H₃); 8.17 (1H, s, H₃); 8.34 (1H, d, ³*J*_{HH} = 5.8 Hz, H₆). ³¹P NMR δ: 30.3. Anal. Calc. for C₅₄H₅₃N₄P₃RuF₆: C, 60.96; H, 4.83; N, 5.27%. Found: C, 60.95; H, 4.94; N, 5.05%. FT-IR/cm⁻¹: 2149s (ν{N≡N}), 2101w (ν{C≡C}).

Crystal structure determinations

Data collection was carried out on a Bruker SMART diffractometer with the crystal mounted in a nitrogen stream at -100 °C or on a Bruker APEX diffractometer with the crystal mounted in a nitrogen stream at -173 °C. Structures were solved by direct methods and refined by full-matrix least-squares techniques against *F*² using the programs SHELXS-97¹³ and SHELXL-97.¹⁴ The asymmetric unit of the structure of **3b**·3C₇H₈ contains two half molecules of toluene solvent that are badly disordered about inversion centres, which have been refined isotropically without the addition of hydrogen atoms. There are also two fully ordered toluene molecules that have been refined anisotropically with hydrogen atoms. The crystal structure of **3c**·2.5C₇H₈ has *Z*' = 2, so the asymmetric unit contains two molecules of **3c** and five of toluene. In one of the PPh₃ ligands of one of these two molecules of **3c** two of the phenyl rings are each disordered equally over two sites.

Crystal data. **3b**·3C₇H₈·C₈₃H₆₀Br₂N₄O₄P₂Ru: *M* = 1500.18, triclinic, space group *P*1 (no. 2), *a* = 11.939(3), *b* = 13.588(2), *c* = 24.678(4) Å, *a* = 82.868(17), *β* = 84.101(16), *γ* = 64.082(15)°, *U* = 3567.6(12) Å³, *T* = 173(2) K, λ = 0.71073 Å, *Z* = 2, μ(Mo-Kα) = 1.439 mm⁻¹, 44608 reflections measured, 16145 unique (*R*_{int} = 0.0607), *R*₁ [*I* > 2σ(*I*)] = 0.0503, *R*₁ [all data] = 0.1084.

3c·2.5C₇H₈: C_{79.5}H₆₄I₂N₄O₄P₂Ru, *M* = 1556.16, triclinic, space group *P*1̄ (no. 2), *a* = 15.158(3), *b* = 20.783(4), *c* = 21.935(4) Å, *a* = 90.29(3), *β* = 92.81(3), *γ* = 100.88(3)°, *U* = 6777(2) Å³, *T* = 100(2) K, *λ* = 0.71073 Å, *Z* = 4, *μ*(Mo-Kα) = 1.244 mm⁻¹, 68419 reflections measured, 30886 unique (*R*_{int} = 0.0299), *R*₁ [*I* > 2σ(*I*)] = 0.0587, *R*₁ [all data] = 0.0782.

3c·CH₂Cl₂: C₆₃H₄₆Cl₂I₂N₄O₄P₂Ru, *M* = 1410.75, monoclinic, space group *P*2₁/*c* (no. 14), *a* = 18.979(2), *b* = 13.4126(18), *c* = 22.890(3) Å, *β* = 101.9882(8)°, *U* = 5699.6(12) Å³, *T* = 100(2) K, *λ* = 0.71073 Å, *Z* = 4, *μ*(Mo-Kα) = 1.561 mm⁻¹, 40 426 reflections measured, 13 089 unique (*R*_{int} = 0.0656), *R*₁ [*I* > 2σ(*I*)] = 0.0426, *R*₁ [all data] = 0.0731.

4·CH₂Cl₂: C₅₅H₅₃Cl₂F₆N₄P₃Ru, *M* = 1148.89, monoclinic, space group *P*2₁/*c* (no. 14), *a* = 16.692(6), *b* = 11.874(4), *c* = 26.902(8) Å, *β* = 97.69(3)°, *U* = 5284(3) Å³, *T* = 173(2) K, *λ* = 0.71073 Å, *Z* = 4, *μ*(Mo-Kα) = 0.551 mm⁻¹, 33 710 reflections measured, 12 121 unique (*R*_{int} = 0.0866), *R*₁ [*I* > 2σ(*I*)] = 0.0663, *R*₁ [all data] = 0.1372.

CCDC reference numbers 246092–246095.

See <http://www.rsc.org/suppdata/dt/b4/b411609g/> for crystallographic data in CIF or other electronic format.

Z-Scan studies

Z-Scans were recorded for solutions of the samples in dichloromethane with concentrations in the range 0.5–4% w/w. Most experiments were performed at 800 nm using an amplified Ti-sapphire laser system delivering μJ range pulses of *ca.* 150 fs duration at a repetition rate of 30 Hz. Samples for Z-scan were placed in 1 mm path glass cells and the scans were recorded using an *f* = 275 mm lens providing a focal plane spot size of about *w*₀ = 42 μm. The light intensity was adjusted to keep the nonlinear phase shift in the solvent cell and cells with solutions in the Δφ₀ = 0.5–1 rd range (roughly on the order of 100 GW cm⁻²). The phase shifts and the imaginary (absorptive) parts of the nonlinearity were obtained by numerical fitting of both closed aperture and open aperture Z-scan traces and the absolute values were determined using a comparison with Z-scans on a 1 mm thick silica plate for which the nonlinear refractive index *n*₂ = 3 × 10⁻¹⁶ cm² W⁻¹ was assumed.

In addition, Ru(Me₂bipy)(PPh₃)₂(-C≡CPh)Cl was also investigated at 670 nm. This wavelength was obtained from another amplified femtosecond system comprising a Clark MXR CPA-2001 regenerative amplifier and a Light Conversion TOPAS optical parametric amplifier. This system was operated at the repetition rate of 250 Hz and the beam parameters were similar to those for 800 nm measurements (*w*₀ = 50 μm was used).

Results and discussion

Synthesis of new alkynyl compounds

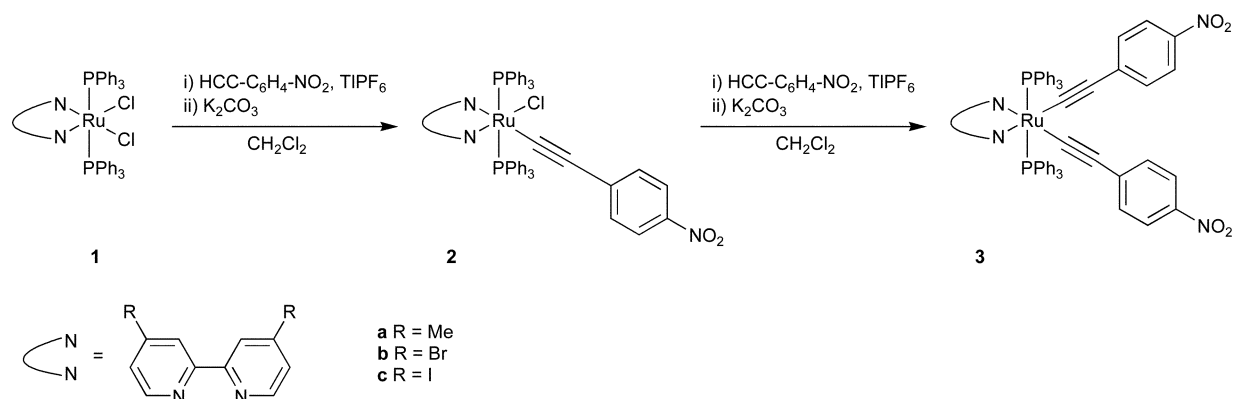
In order to discover whether bis-alkynyl compounds of the general formula Ru(Me₂bipy)(PPh₃)₂(-C≡CR)₂ could

be synthesised, the reaction of the mono-alkynyl compounds Ru(Me₂bipy)(PPh₃)₂(-C≡CR)Cl (*R* = Bu^t, C₆H₄Me-*p*, C₆H₄NO₂-*p* **2a**) with further terminal alkyne in the presence of TIPF₆ and K₂CO₃ was investigated. We have reported the preparation of the first two of these mono-alkynyl starting materials previously, and that of the third, Ru(Me₂bipy)(PPh₃)₂(-C≡CC₆H₄NO₂-*p*)Cl **2a** from the dichloride Ru(Me₂bipy)(PPh₃)₂Cl₂ **1a** is given herein. Although this preparation is analogous to those previously published, replacement of a chloride ligand with an alkyne (as a vinylidene ligand) and subsequent deprotonation, the synthesis has been modified to allow a one-pot procedure without isolation of the intermediate vinylidene compound (Scheme 1).

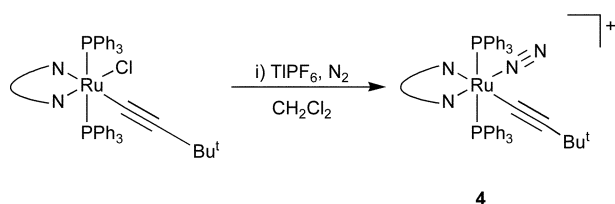
The formation of the bis-alkynyl compound Ru(Me₂bipy)(PPh₃)₂(-C≡CC₆H₄NO₂-*p*)₂ **3a** from **2a** may indeed be achieved in the same manner as that of **2a** from **1a** (Scheme 1), although the first half of the reaction proceeds more slowly; only after reaction for two days (*cf.* 2 h) is complete replacement of chloride by vinylidene achieved. **2a** and **3a** display more absorption bands (two and three respectively) in the C≡C region of the IR spectrum than there are carbon-carbon triple bonds, because of Fermi coupling¹⁵ – the same is also true of Ru(Me₂bipy)(PPh₃)₂(-C≡CC₆H₄Me-*p*)Cl.¹ In contrast, the attempted synthesis of Ru(Me₂bipy)(PPh₃)₂(-C≡CC₆H₄Me-*p*)₂ from Ru(Me₂bipy)(PPh₃)₂(-C≡CC₆H₄Me-*p*)Cl by the same method was not possible. It appears to be the formation of the intermediate mixed vinylidene-alkynyl complex that is unsuccessful; although a white precipitate of TiCl₄ is observed in the reaction vessel, the resulting solution contains a multitude of ³¹P NMR signals.

Preparation of Ru(Me₂bipy)(PPh₃)₂(-C≡CBu^t)₂ by the same method was also unsuccessful, although in this case ³¹P NMR reveals a relatively clean reaction. Isolation of the product and subsequent characterisation reveals it to be [Ru(Me₂bipy)(PPh₃)₂(-C≡CBu^t)(N≡N)][PF₆]**4**, in which the chloride ligand of the starting material has been replaced not with a molecule of *tert*-butylacetylene but with one of dinitrogen (Scheme 2). The reason for this is presumably steric; inspection of the crystal structure of Ru(Me₂bipy)(PPh₃)₂(-C≡CBu^t)Cl¹ reveals that even after the chloride ligand has been eliminated there is little space in the coordination sphere of the metal for the η²-coordination of another alkyne molecule that precedes isomerisation to a vinylidene group. The IR spectrum of **4** contains two bands in the triple bond region, a strong one at 2146 cm⁻¹ and a weak one at 2101 cm⁻¹. These may be assigned by synthesising **4** under an atmosphere of ¹⁵N₂, which leads to the appearance of a strong new absorption at 2073 cm⁻¹. This is the correct position to be the counterpart of the absorption at 2146 cm⁻¹, which is therefore ν(N≡N), and so the absorption at 2101 cm⁻¹ is ν(C≡C). This is consistent with the observation that N≡N absorptions tend to be strong.¹⁶

A crystal suitable for X-ray diffraction was grown from a dichloromethane-hexane solution of **4**, and the cation of



Scheme 1 Synthesis of compounds **2** and **3**.

Scheme 2 Synthesis of **4**⁺.

the resulting structure is shown in Fig. 1. Selected bond lengths and angles are presented in Table 1, and show that the geometry of the ruthenium centre is much more similar to that of the (neutral) ruthenium(II) complex $\text{Ru}(\text{Me}_2\text{bipy})(\text{PPh}_3)_2(-\text{C}\equiv\text{CBu}^t)\text{Cl}$ than to that of the (cationic) ruthenium(III) compound $[\text{Ru}(\text{Me}_2\text{bipy})(\text{PPh}_3)_2(-\text{C}\equiv\text{CBu}^t)\text{Cl}][\text{PF}_6]$.¹ For example, the distances $\text{Ru}(1)-\text{C}(13)$, $\text{C}(13)-\text{C}(14)$ and $\text{Ru}(1)-\text{N}(1)$ of 2.032(5), 1.179(7) and 2.124(4), respectively, in **4** are well matched by those of 2.053(5), 1.174(6) and 2.120(4) in $\text{Ru}(\text{Me}_2\text{bipy})(\text{PPh}_3)_2(-\text{C}\equiv\text{CBu}^t)\text{Cl}$,¹ which seems to imply that it is the oxidation state of the metal rather than the charge of the complex that is more important in determining these bond lengths.

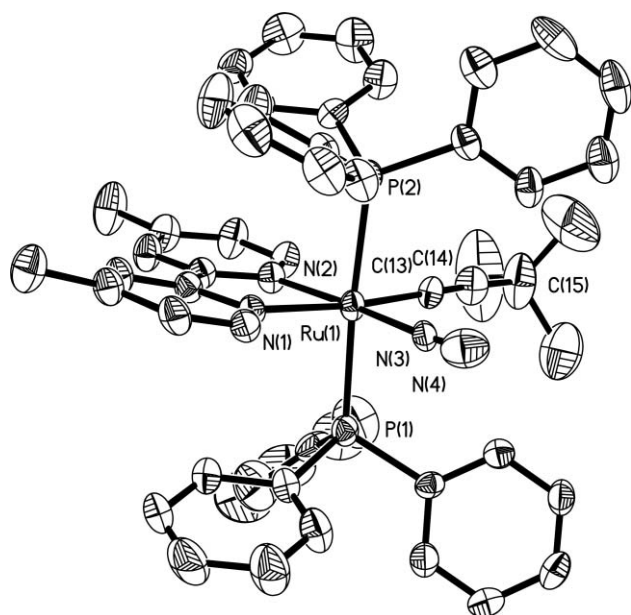


Fig. 1 ORTEP (50% probability level) of **4**⁺. Hydrogen atoms have been removed for clarity.

The $\text{N}\equiv\text{N}$ bond distance of 1.011(6) Å seen in the structure of **4** is among the shortest observed in ruthenium–dinitrogen compounds. A search of the Cambridge Structural Database¹⁷ shows that it contains 13 other mono-ruthenium compounds with a σ -bonded, non-bridging, dinitrogen ligand. Within experimental error, 11 of these possess $\text{N}\equiv\text{N}$ distances of around 1.08–1.11 Å, comparable to the distance observed in free N_2 (1.097 Å).¹⁸ However, there are two complexes that show short $\text{N}\equiv\text{N}$ distances of around 1.01 Å like **4**, which are $[\text{RuTp}(\text{PET}_3)_2(\text{N}_2)][\text{BPh}_4]$ ¹⁹ (Tp = hydrotris(pyrazolyl)borate) {1.01(2) Å} and $[\text{Ru}(16\text{-TMC})(\text{N}_2)\text{Cl}][\text{PF}_6]$ ²⁰ (16-TMC = 1,5,9,13-tetramethyl-1,5,9,13-

Table 1 Selected bond lengths and angles in the structure of **4**⁺

$\text{Ru}(1)-\text{N}(3)$	1.994(5)	$\text{Ru}(1)-\text{P}(1)$	2.3769(17)
$\text{Ru}(1)-\text{C}(13)$	2.032(5)	$\text{Ru}(1)-\text{P}(2)$	2.4010(17)
$\text{Ru}(1)-\text{N}(2)$	2.084(4)	$\text{C}(13)-\text{C}(14)$	1.179(7)
$\text{Ru}(1)-\text{N}(1)$	2.124(4)	$\text{N}(3)-\text{N}(4)$	1.011(6)
$\text{N}(3)-\text{Ru}(1)-\text{C}(13)$	94.79(19)	$\text{C}(14)-\text{C}(13)-\text{Ru}(1)$	177.0(5)
$\text{P}(1)-\text{Ru}(1)-\text{P}(2)$	176.29(5)		

tetraazacyclohexadecane) {1.005(10) Å}. The fact that the $\text{N}\equiv\text{N}$ distance does not normally vary much from the free gas has been interpreted by invoking contributions from two opposing effects of approximately equal magnitude – donation from a σ^* lone-pair on the dinitrogen to the metal, which causes the $\text{N}\equiv\text{N}$ distance to decrease by removing electron density from an antibonding orbital, and back donation from the metal into the π^* orbitals of the dinitrogen, which causes the $\text{N}\equiv\text{N}$ distance to increase.²¹ The shortness of the $\text{N}\equiv\text{N}$ distance in **4** implies that this back-bonding contribution is very small, although why this should be the case is not apparent; though $[\text{RuTp}(\text{PET}_3)_2(\text{N}_2)]^+$, $[\text{Ru}(16\text{-TMC})(\text{N}_2)\text{Cl}]^+$ and **4**⁺ are all cationic, octahedral, d^6 ruthenium(II) fragments, the same is also true of other fragments which do not show the same shortening of the $\text{N}\equiv\text{N}$ bond.

Spectroscopic behaviour

We have previously shown that in the mono-alkynyl compounds $\text{Ru}(\text{Me}_2\text{bipy})(\text{PPh}_3)_2(-\text{C}\equiv\text{CR})\text{Cl}$ ($\text{R} = \text{Bu}^t, \text{Ph}, p\text{-C}_6\text{H}_4\text{Me}$), the HOMO is a metal t_{2g} -derived orbital and the LUMO is a π^* orbital on the bipyridine. The lowest energy band seen in their UV/visible spectra is thus metal to bipyridine MLCT in nature, appearing at around 490–500 nm with an extinction coefficient in the order of $10^3 \text{ M}^{-1} \text{ cm}^{-1}$.¹ The spectra of compounds **2** and **3** also have a lowest energy band in approximately the same position, but this is much broader and an order of magnitude stronger ($\epsilon \approx 10^4 \text{ M}^{-1} \text{ cm}^{-1}$), indicating that it has a different origin (below).

The HOMOs of compounds **1a**, **2a** and **3a** are metal based, as before. These compounds all show Ru^{II} to Ru^{III} oxidations at relatively low (<0.6 V vs. SCE) potentials, and the ESR spectra of samples of the representative compounds **2a**⁺ and **3a**⁺ (generated *in situ* by oxidation of the neutral compound with ferrocenium hexafluorophosphate) show the rhombic pattern† typical of similar compounds.^{1–22} Oxidising these compounds creates a vacancy in the d_{xy} orbital of the metal,¹ causing their colour to change as an alkynyl-to-metal LMCT band appears. This has been investigated using UV/visible spectroelectrochemistry for **2a** and **3a**, and the results for **3a** are shown in Fig. 2. Upon generation of **3a**⁺ the broad band observed between 400 and 700 nm in the spectrum of **3a** disappears and is replaced by several other features, notably a band of medium strength at around 400 nm, and two LMCT features at 740 ($\epsilon \approx 6532 \text{ M}^{-1} \text{ cm}^{-1}$) and 798 nm ($\epsilon \approx 6662$). Analogous bands are also present in the spectrum of electrochemically generated **2a**⁺, at 611 ($\epsilon \approx 2101$) and 678 nm ($\epsilon \approx 3395$).

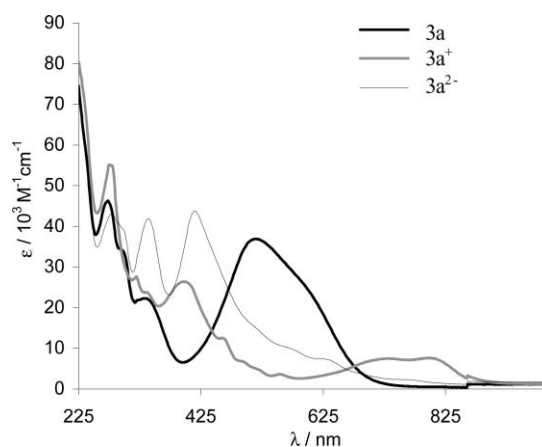


Fig. 2 The UV/visible spectra of compound **3a** before and after oxidation and reduction.

† For **2a**⁺, $g_1 = 2.292$, $g_2 = 2.260$ and $g_3 = 1.891$. For **3a**⁺, $g_1 = 2.358$, $g_2 = 2.272$ and $g_3 = 1.860$.

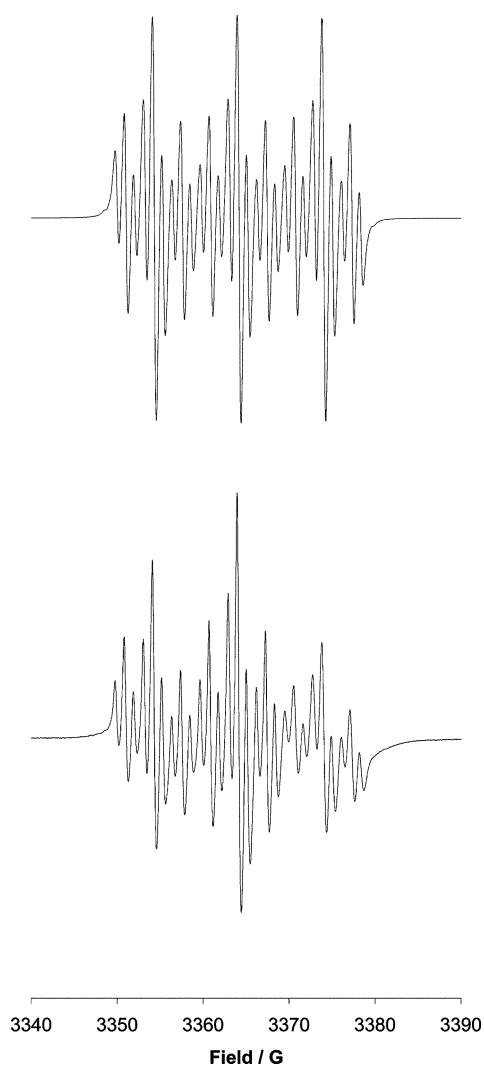


Fig. 3 Simulated (top) and observed (bottom) ESR spectra of $3a^{2-}$.

Unlike the mono-alkynyl complexes $Ru(Me_2bipy)(PPh_3)_2(-C\equiv CR)Cl$ ($R = Bu^t, Ph, p-C_6H_4Me$), the LUMO of compounds **2a** and **3a** is not bipyridyl based. Cyclic voltammetry reveals that they each have a reversible reduction wave at around -1.20 V vs. SCE that is not displayed by the aforementioned mono-alkynyl compounds, and this is due not to the reduction of a bipyridyl π^* based LUMO, but of a π^* LUMO (or two degenerate LUMOs in the case of **3a**) based on the nitrophenyl group(s) of the alkynyl ligand. This is confirmed by the ESR spectrum displayed by an electrochemically reduced sample of **3a**, which shows coupling to one nitrogen atom and to two pairs of protons (Fig. 3 and Table 2), unequivocally confirming the nitrophenyl groups as the location of the reduction, since reduced bipyridyl ligands show a five line pattern due to coupling to two nitrogen nuclei. Upon reduction, **2a** and **3a** therefore behave similarly to the platinum bis-alkynyl compound $Pt^t(Bu_2bipy)(-C\equiv CC_6H_4NO_2)_2$ that we have reported on previously.²³ This too has two degenerate nitrophenyl-based LUMOs that are populated upon reduction, and also displays a diagnostic ESR pattern.

Table 2 Parameters used for simulating the ESR spectrum of $3a^{2-}$ shown in Fig. 3. A Lorentzian linewidth of 0.45 G and a g value of 2.0155 were used

Nucleus	No. of nuclei	a/G
^{14}N	1	9.856
1H	2	3.278
1H	2	1.052
$^{99, 101}Ru$	1	0.53

The UV/visible spectrum of electrochemically reduced **3a** is also shown in Fig. 2, which again shows the loss of the broad band observed between 400 and 700 nm in the spectrum of **3a** and the production of several new features. Particularly strong are two bands at 339 and 415 nm, each with $\epsilon \approx 40000$; the former of these is characteristic of reduced *para*-substituted nitrobenzenes.²⁴

Given the nature of the HOMOs and LUMOs of **2** and **3**, the broad, intense band visible in their UV/visible spectra between about 400 and 700 nm is thus either metal-to-nitro charge transfer, or more probably (given the distance between metal and nitro group) a nitrophenylalkynyl localised $\pi-\pi^*$ band.²⁵ This latter hypothesis is supported by the fact that upon adding a second such ligand (*i.e.* on moving from **2** to **3**), the strength of the absorption increases by a factor of approximately 2. Judged by the similarity of their UV/visible spectra this is true of all six of the nitro-alkynyl compounds reported herein, although it is worth noting that compounds **2b**, **2c**, **3b** and **3c** (*vide infra*) show only irreversible cathodic processes in the cyclic voltammogram.

Nonlinear optical studies

Because a large number of ruthenium compounds containing nitro-substituted arylalkynyl ligands show non-linear optical activity,²⁶ compounds $Ru(Me_2bipy)(PPh_3)_2(-C\equiv CR)Cl$ ($R = C_6H_4NO_2$, **2a**, Bu^t , Ph , C_6H_4Me) were investigated for non-linear optical response at 800 nm. Cubic optical non-linearities were determined by Z-scans, typical traces for the solvent and two concentrations of **2a**, together with theoretical curves, being shown in Fig. 4. The deviations of Z-scans from that predicted by theory that are seen in the wing regions are due to some non-Gaussian character of the beam which, however, does not influence the accuracy of the determination of the nonlinear parameters.

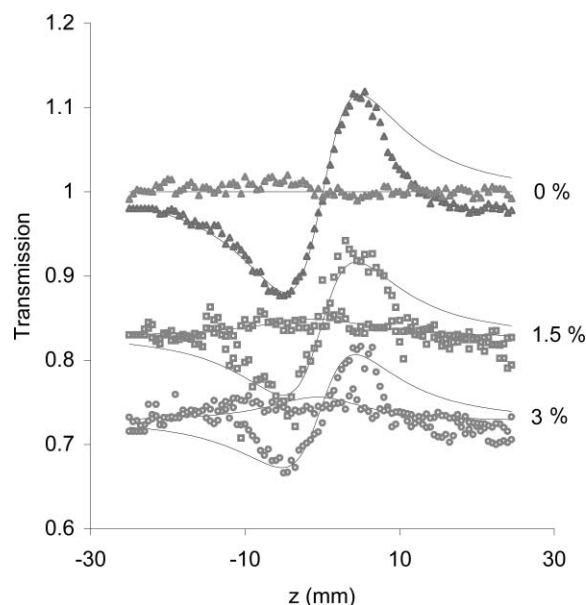


Fig. 4 Closed aperture Z-scans for pure CH_2Cl_2 and 1.5 and 3% solutions of **2a**. Wavelength = 800 nm, pulse duration *ca.* 150 fs.

Table 3 lists the real (γ_{real}) and imaginary (γ_{imag}) parts of the cubic hyperpolarizability obtained from these studies. It should be stressed that, primarily because of the limited range of concentrations that were available, the results for two of the compounds ($R = p-C_6H_4Me, Bu^t$) have error brackets that are too high to be of use. For the remaining two compounds ($R = p-C_6H_4NO_2$, **2a**, Ph), the estimates of the real part of γ are of the order of 10^{-34} esu, which indicates moderate nonlinearities. The imaginary parts of the nonlinearities are negligible (*i.e.* two-photon absorption at 800 nm is quite weak), except for **2a**, which has a relatively pronounced absorptive nonlinearity at 800 nm,

Table 3 Cubic nonlinear optical data for Ru(Me₂bipy)(PPh₃)₂(–C≡CR)Cl. Results of Z-scan measurements at 800 nm in CH₂Cl₂ (except * at 670 nm)

R	$\gamma_{\text{real}}/10^{-36}$ esu	$\gamma_{\text{imag}}/10^{-36}$ esu
<i>p</i> -C ₆ H ₄ NO ₂ 2a	–200 ± 30	–65 ± 4
<i>p</i> -C ₆ H ₄ Me	110 ± 200	2 ± 3
Ph	100 ± 30	7 ± 2
Ph	–1070 ± 300*	13 ± 8*
Bu ^t	280 ± 200	10 ± 3

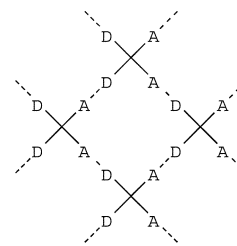
its negative sign indicating that the effect is of the induced transmission type rather than the two-photon absorption type as for the other compounds. Indeed, **2a** shows some one-photon absorption at 800 nm and absorption saturation effects are seen. The origin of the absorption is not clear, however, it could be a tail of short-wavelength absorption or it could result from some oxidation of the compound. The data for these compounds are similar in magnitude to previously-reported ruthenium acetylide complexes of comparable size.²⁷

The data for Ru(Me₂bipy)(PPh₃)₂(–C≡C–Ph)Cl at 670 nm were obtained under conditions of relatively strong one-photon absorption. From comparison with the 800 nm data for the same compound, the change of sign of the nonlinearity and increase of its absolute value may be postulated to be an effect of moving the wavelength closer to a resonance.

Crystal engineering

There have been several papers published recently concerning the crystal structures of organic compounds containing both nitro and iodo functionalities.²⁸ It has been demonstrated that the polarisation-assisted attractive interaction between the two is strong enough to influence the packing of molecules in the solid state, and in particular the elegant work of Desiraju and co-workers has shown how pre-defined packing geometries may be achieved, since molecules tend to adopt an arrangement that reflects the disposition of the two halves of the synthon. Thus, to take just three examples, the crystal structures of *para*-iodonitrobenzene and 4-iodo-4'-nitrobiphenyl, where the iodo and nitro groups in each molecule are at 180° to each other, contain linear chains of molecules linked by iodo–nitro interactions,²⁹ whereas that of 4,4'-diiodo-4'',4'''-dinitrotetraphenylmethane, in which two iodo and two nitro groups are arranged tetrahedrally around a carbon centre, contains a diamondoid network.³⁰ Although less commonly used for crystal engineering than iodo–nitro interactions, bromo–nitro interactions have also been shown to have the capacity for structure direction.³¹

All previous work that has used halo–nitro interactions for crystal engineering has concerned purely organic systems. How-

**Fig. 5** A cruciform donor (D)–acceptor (A) system can lead to a polar two-dimensional sheet of molecules.

ever, we reasoned that the ruthenium bis-nitrophenylalkynyl systems reported above could provide a pathway into crystal engineering using coordination compounds. Making such a compound with a 4,4'-dihalobipyridine would create a cruciform donor–acceptor system in the equatorial plane of the molecule, which could cause it to form a two-dimensional network in the solid state (Fig. 5). We were also interested in investigating whether the attractive intermolecular forces that could cause relatively small organic molecules to aggregate as described above would be strong enough to influence the packing of much larger metal-containing molecules, where such forces would contribute a much smaller fraction of the total lattice energy.

The synthesis of Ru(Br₂bipy)(PPh₃)₂(–C≡CC₆H₄NO₂)₂ **3b** was readily achieved from the corresponding dichloride **1b** via the mono-alkynyl compound **2b**, using the procedure described above for the synthesis of **3a** from **1a**. Crystals suitable for X-ray diffraction were grown from a refrigerated toluene solution; the resulting structure of **3b** is shown in Fig. 6, and selected bond lengths and angles are presented in Table 4. Whilst this structure confirms the general geometry of the compound – *cis*-alkynyl and *trans*-triphenylphosphine ligands–examination of the packing reveals that there are no interactions between the bromo and nitro groups.

Though 4,4'-diiodo-2,2'-bipyridine (I₂bipy) has not been reported before, 4-iodopyridine is readily synthesised from 4-aminopyridine via a Sandmeyer reaction.¹² This procedure also works when applied to 4,4'-diamino-2,2'-bipyridine, yielding I₂bipy as a stable, crystalline white solid. As expected, this readily coordinates to ruthenium, and the synthesis of Ru(I₂bipy)(PPh₃)₂(–C≡CC₆H₄NO₂)₂ **3c** was achieved in an analogous way to **3a** and **3b**. The first crystals of **3c** for X-ray diffraction were grown by refrigeration of a toluene solution. The asymmetric unit of the crystal structure (hereafter referred to as structure A) contains two crystallographically independent molecules of **3c** and five of toluene. Generally the bond lengths and angles observed within the two independent molecules are similar to each other and to the corresponding value in the structure of **3b** (Table 4), but a striking exception is the angle comprised of the two atoms of the carbon–carbon triple bond

Table 4 Selected bond lengths (Å) and angles (°) in the structures of compounds **3b** and **3c**. Structure A of the latter has two independent molecules in the asymmetric unit, and thus has two values for each measurement

	3b	3c	
		Structure A	Structure B
Ru(1)–N(1)	2.114(3)	2.104(4)	2.137(4)
Ru(1)–N(2)	2.111(3)	2.123(4)	2.117(4)
Ru(1)–C(11)	1.991(4)	1.993(5)	1.986(4)
Ru(1)–C(19)	1.984(4)	1.985(5)	1.999(4)
C(11)–C(12)	1.216(5)	1.206(7)	1.220(6)
C(19)–C(20)	1.220(5)	1.210(7)	1.213(6)
Ru(1)–C(11)–C(12)	174.8(3)	177.9(4)	177.5(4)
C(11)–C(12)–C(13)	176.3(4)	171.8(6)	168.4(5)
Ru(1)–C(19)–C(20)	176.7(3)	178.0(5)	175.1(4)
C(19)–C(20)–C(21)	177.1(4)	170.2(5)	177.3(5)
P(1)–Ru(1)–P(2)	173.72(4)	171.71(5)	171.33(4)
			173.98(4)

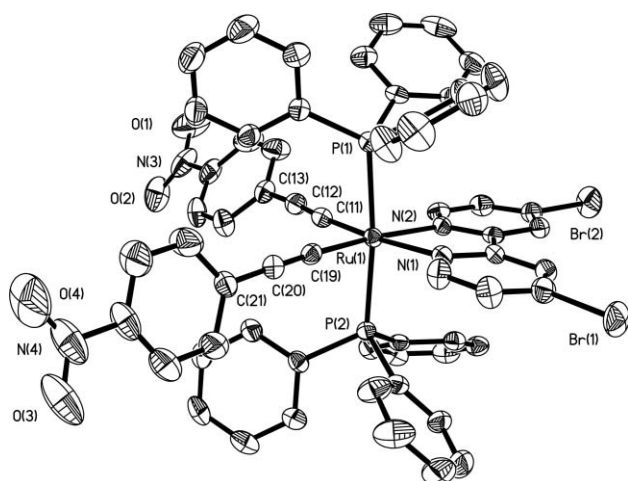


Fig. 6 ORTEP (50% probability level) of the structure of **3b**. Hydrogen atoms have been removed for clarity.

and the *ipso* carbon atom of the nitrophenyl ring, varying from $177.3(4)^\circ$ in one molecule to $168.4(5)^\circ$ in the other.

Examination of the packing within structure A of **3c** reveals that it does contain iodo–nitro interactions that orient the molecules. However, instead of the envisaged two-dimensional network, two separate one-dimensional chains running in opposite directions are observed, each comprised of one of the two different molecules of **3c** (Fig. 7). This is due to the nature of the iodo–nitro interaction seen (Table 5), which links molecules together in a convergent, rather than divergent, fashion. Somewhat unusually, the iodo atoms are not in the plane of the nitro group, which is by far the most common angle of interaction,²⁸ but are almost perpendicular to it. It is this feature that allows the convergence of the two interactions between the donor and acceptor molecules and leads to chains rather than sheets.

As the iodo–nitro interaction in structure A of **3c** is rather atypical, and because of the presence of several molecules of toluene, a second set of crystals (as a dichloromethane solvate) for X-ray diffraction were grown from a different solvent system (layered dichloromethane–hexane). The metrics of **3c** within structure B are very similar to those within structure A (Table 4), but unlike structure A, structure B contains no short iodo–nitro interactions. It does, however, have a 3 \AA contact (Fig. 8) between the acidic hydrogen atom of the CH_2Cl_2 solvent molecule and the triple bond of the alkynyl ligand, of the type recently noted.²

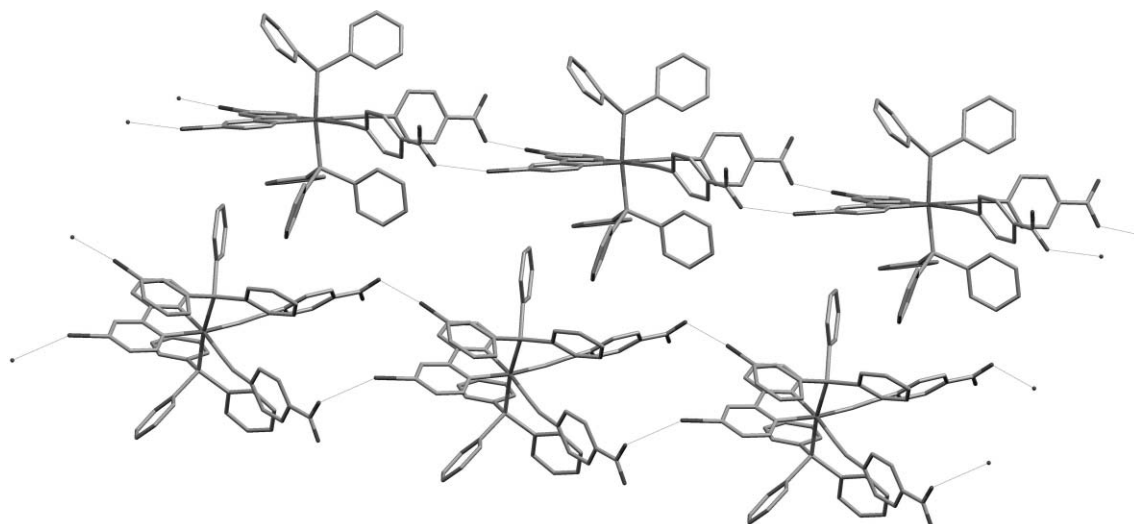


Fig. 7 Chains of molecules with iodo–nitro interactions in structure A of **3c**. Each chain is composed solely of one of the two independent molecules in the asymmetric unit.

Table 5 Iodo–oxygen distances (\AA) seen in structure A of **3c**, illustrating the unsymmetric nature of the iodo–nitro interaction. The sum of the van der Waals' radii of iodine and oxygen is 3.50 \AA , and thus the shorter iodo–oxygen contacts d_1 constitute stabilising interactions. The angle χ is the torsion angle $\text{O}_2\text{--N--O}_1\text{--I}$; in other words, the angle of elevation of the iodo group from the planar nitro group

Molecule	d_1	d_2	χ
1	3.126	4.743	75.09
1	2.924	3.929	78.09
2	3.107	4.775	80.00
2	3.272	4.115	83.14

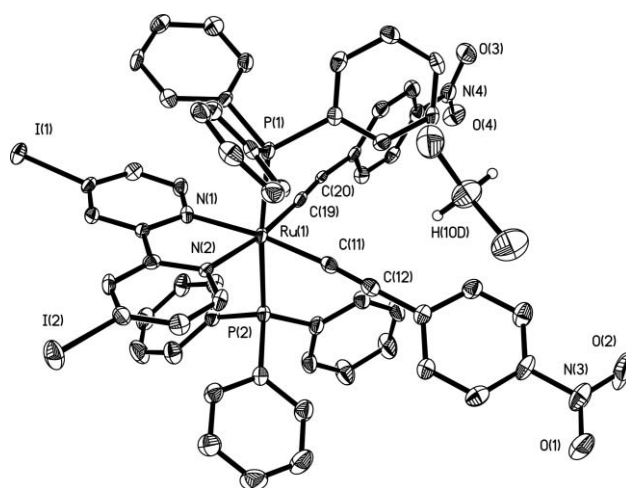
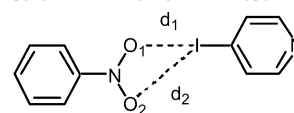


Fig. 8 ORTEP (50% probability level) of **3c** from structure B, showing that the dichloromethane solvent molecule is oriented to allow H(10D) to interact with the C(11)–C(12) triple bond. Most hydrogen atoms have been removed for clarity.

Conclusions

The results obtained for the reactions of the ruthenium mono-alkynyl complexes with further alkyne in the presence of TIPF_6 allow us to draw some conclusions regarding the stability of the desired compounds. Both *p*-nitrophenylacetylene and *p*-tolylacetylene are of similar size, yet the alkynyl compound **2** of the former readily forms an alkynyl–vinylidene complex

(which is then converted *in-situ* to the bis-alkynyl complex **3**) whilst the latter does not, implying that an electronic factor can account for the difference. As *p*-tolylacetylene is a much better electron donor than *p*-nitrophenylacetylene, it seems that electron-withdrawing groups can stabilise this alkynyl–vinylidene intermediate and allow subsequent synthesis of bis-alkynyl compounds, a hypothesis that is currently under investigation in our laboratory. *tert*-Butylacetylene is both a better electron donor and much bulkier than the aforementioned arylalkynes; under the above postulate, the former property implies that the alkynyl–vinylidene intermediate would not be stable, but the latter property seems to prevent formation of this in the first place, and rather than fit another bulky ligand around the metal a sterically undemanding dinitrogen ligand is incorporated instead.

In having a low-lying π^* orbital the nitrophenylalkynyl ligand is not typical of the majority of arylalkynyl ligands. The consequence of this is that the optical properties of the bis(nitrophenylalkynyl) ruthenium compounds reported herein are probably not going to be the same as those of similar compounds with other ligands.

Our foray into crystal engineering has also produced some interesting results. Not the least of these is the first synthesis of 4,4'-diiodo-2,2'-bipyridine, which the weakness of the carbon–iodine bond makes a potentially valuable precursor to 4,4'-disubstituted bipyridines. However, using it to interact with nitro-containing alkynyl ligands has been less successful. Although structure A of **3c** does contain short iodo-nitro contacts, structure B does not, and furthermore the non-planarity of the iodo-nitro interaction in structure A is not typical of that normally observed when using it for the construction of a supramolecular motif. This leads us to conclude that the strength of this interaction is probably not great enough to be structure determining in the current system, and that its presence in structure A, although probably attractive in nature, is not the major influence on the packing geometry.

Acknowledgements

C. J. A. thanks the University of Bristol for a Junior Fellowship, and M. G. H. thanks the Australian Research Council for an ARC Australian Professorial Fellowship.

References

- 1 C. J. Adams and S. J. A. Pope, *Inorg. Chem.*, 2004, **43**, 3492.
- 2 W. Lu, M. C. W. Chan, N. Zhu, C.-M. Che, Z. He and K.-Y. Wong, *Chem. Eur. J.*, 2003, 6155.
- 3 A. B. Pangborn, M. A. Giardello, R. H. Grubbs, R. K. Rosen and F. J. Timmers, *Organometallics*, 1996, **15**, 1518.

- 4 P. S. Hallman, T. A. Stephenson and G. A. Wilkinson, *Inorg. Synth.*, 1970, **12**, 237.
- 5 C. J. Adams, *J. Chem. Soc., Dalton Trans.*, 2002, 1545.
- 6 G. Maerker and F. H. Case, *J. Am. Chem. Soc.*, 1958, **80**, 2745.
- 7 G.-J. ten Brink, I. W. C. E. Arends, M. Hoogenraad, G. Verspui and R. A. Sheldon, *Adv. Synth. Catal.*, 2003, **345**, 497.
- 8 S. Takahashi, Y. Kuroyama, K. Sonogashira and N. Hagihara, *Synthesis*, 1980, 627.
- 9 N. G. Connelly and W. E. Geiger, *Chem. Rev.*, 1996, **96**, 877.
- 10 S.-M. Lee, R. Kowallick, M. Marcaccio, J. A. McCleverty and M. D. Ward, *J. Chem. Soc., Dalton Trans.*, 1998, 3443.
- 11 A. Hilton, T. Renouard, O. Maury, H. L. Bozec, I. Ledoux and J. Zyss, *Chem. Commun.*, 1999, 2521.
- 12 C. Coudret, *Synth. Commun.*, 1996, **26**, 3543.
- 13 G. M. Sheldrick, *SHELXS-97, Program for Crystal Structure Determination*, University of Göttingen, 1997.
- 14 G. M. Sheldrick, *SHELXL-97, Program for Crystal Structure Refinement*, University of Göttingen, 1997.
- 15 R. Denis, L. Toupet, F. Paul and C. Lapinte, *Organometallics*, 2000, **19**, 4240; F. Paul, J.-Y. Mevellec and C. Lapinte, *J. Chem. Soc., Dalton Trans.*, 2002, **19**, 1783.
- 16 B. Folkesson, *Acta Chem. Scand.*, 1972, **26**, 4008.
- 17 F. H. Allen, *Acta Crystallogr., Sect. B*, 2002, **58**, 380.
- 18 P. G. Wilkinson and N. B. Houk, *J. Chem. Phys.*, 1956, **24**, 528.
- 19 M. A. J. Tenorio, M. J. Tenorio, M. C. Puerta and P. Valerga, *J. Chem. Soc., Dalton Trans.*, 1998, 3601.
- 20 W.-H. Chiu, C.-M. Che and T. C. W. Mak, *Polyhedron*, 1996, **15**, 4421.
- 21 G. Trimmel, C. Slugovc, P. Wiede, K. Mereiter, V. N. Sapunov, R. Schmid and K. Kirchner, *Inorg. Chem.*, 1997, **36**, 1076.
- 22 J. Chakravarty and S. Bhattacharya, *Polyhedron*, 1994, **13**, 2671.
- 23 C. J. Adams, S. L. James, X. Liu, P. R. Raithby and L. J. Yellowlees, *J. Chem. Soc., Dalton Trans.*, 2000, 63.
- 24 R. G. Compton, R. A. W. Dryfe and A. C. Fisher, *J. Chem. Soc., Perkin Trans. 2*, 1994, 1581.
- 25 C. E. Whittle, J. A. Weinstein, M. W. George and K. S. Schanze, *Inorg. Chem.*, 2001, **40**, 4053.
- 26 S. K. Hurst, M. P. Cifuentes, J. P. L. Morrall, N. T. Lucas, I. R. Whittall, M. G. Humphrey, I. Asselberghs, A. Persoons, M. Samoc, B. Luther-Davies and A. C. Willis, *Organometallics*, 2001, **20**, 4664; C. E. Powell and M. G. Humphrey, *Coord. Chem. Rev.*, 2004, **248**, 725.
- 27 I. R. Whittall, M. G. Humphrey, M. Samoc, J. Swiatkiewicz and B. Luther-Davies, *Organometallics*, 1995, **14**, 5493; I. R. Whittall, M. G. Humphrey, M. P. Cifuentes, M. Samoc, B. Luther-Davies, A. Persoons and S. Houbrechts, *Organometallics*, 1997, **16**, 2631.
- 28 F. H. Allen, J. P. M. Lommerse, V. J. Hoy, J. A. K. Howard and G. R. Desiraju, *Acta Crystallogr., Sect. B*, 1997, **53**, 1006.
- 29 J. A. R. P. Sarma, F. H. Allen, V. J. Hoy, J. A. K. Howard, R. Thaimattam, K. Biradha and G. R. Desiraju, *Chem. Commun.*, 1997, 101; V. R. Thalladi, B. S. Goud, V. J. Hoy, F. H. Allen, J. A. K. Howard and G. R. Desiraju, *Chem. Commun.*, 1996, 401.
- 30 R. Thaimattam, C. V. K. Sharma, A. Clearfield and G. R. Desiraju, *Cryst. Growth Des.*, 2001, **1**, 103.
- 31 A. D. Bond, D. A. Haynes and J. M. Rawson, *Can. J. Chem.*, 2002, **80**, 1507.